

A TWO-DIMENSIONAL STUDY TO AID THE PROTOTYPE DESIGNING OF MONO-MODE MICROWAVE BLOOD WARMER

Sushma Kumari, Sujoy Kumar Samanta*

Indian Institute of Technology Patna, Department of Chemical and Biochemical Engineering,
Bihta, Patna – 801106, India

This meticulous analysis was performed to guide in the designing of a prototype mono-mode microwave blood warmer. The interaction of two-dimensional cylindrical blood samples with the microwave was performed through two different techniques i.e., lateral and radial irradiations. The study found the preference for interaction techniques corresponding to different frequencies, intensities, sample sizes and procedure durations. The study of the areal positioning of power and temperature at specific peak points generated the information on warming rate and thermal homogeneity inside the sample. High warming rate along with low thermal non-homogeneity were the chosen criteria to decide the requirement of rotation during the warming procedure. At the frequency of 915 MHz, no rotation was recommended for samples irrespective of sizes for optimal warming. Rotation for small and large samples and no rotation for medium sized samples were recommended to achieve homogeneously warmed human blood samples at the frequency of 2450 MHz. Specific recommendations for different case studies were also made with respect to the sample size, radiation intensity and procedure duration to draw reciprocity amongst them. Considering all the aspects, the present work recommended an efficient way for designing of a prototype for enhanced microwave facilitated intravenous fluid warmer.

Keywords: microwave, 2D cylinder, blood warmer, human blood, lateral/radial irradiations

1. INTRODUCTION

The importance of warm human blood during massive transfusion process and its unavailability in the middle- and low-income countries are subjects of great concern and investigation (Custer et al., 2018; Poder et al., 2016b; Smith and Wagner, 2008; Storch et al., 2019). In the initial days, the transfusion process involved direct transfer of blood from the donor. However, the risks of blood borne diseases, infections and unavailability of large quantity at the time of operations/surgeries led to the method of blood collection and preservation at low temperature (Poder et al., 2016a). Nevertheless, the practice of the transfusion of preserved cold blood demonstrated several complications such as ventricular fibrillation, hemorrhagic shocks, etc. (Boyan, 1964). The erroneous initial procedure of warming human blood involved water bath

* Corresponding author, e-mail: sksamanta@iitp.ac.in

<https://journals.pan.pl/cpe>

Presented at the International Chemical Engineering Conference 2021 (ICHEEC): 100 Glorious Years of Chemical Engineering and Technology, held from September 16–19, 2021 at Dr B. R. Ambedkar National Institute of Technology, Jalandhar, Punjab, India.



warming which was prone to bacterial sepsis and long procedure duration (Frazier et al., 2017; Zimrin and Hess, 2009). The desired features in a blood warming process include it being swift, cheap along with ensuring the quality and sterility of the warmed blood (Nair et al., 2021; Smith and Wagner, 2008).

The microwave comes under the non-ionizing category of electromagnetic radiation with the frequency ranging between 0.3 to 300 GHz in the electromagnetic spectrum (Ayappa et al., 1992; Samanta and Basak, 2009). The effect of interaction between the microwave radiation and a dielectric sample is based on the dielectric constant and loss properties of the sample which also result in their volumetric processing (Ayappa et al., 1992; Samanta et al., 2009; 2010). The conversion of electromagnetic energy into heat is decided by the loss factors of the samples being subjected to the microwave radiation. This thermal behavior of the microwave radiation leads to its various applications in the industries like food, polymer, ceramics, material, pharmaceutical, medical sciences, etc. (Kumari and Samanta, 2022a; 2022b; Rosen et al., 2002; Samanta and Basak, 2008; 2010; Vrba, 2005).

The various medical applications of the microwave radiation include tumor ablation, blood and intravenous fluid warming, endometrial ablation, etc. (Lubner et al., 2010; Poder et al., 2016a; Storch et al., 2019). The initial application of microwave for human blood warming displayed the procedure to be very swift in terms of consuming only few minutes (1–3 minutes), whereas conventional methods used to take 30–45 minutes (Hirsch et al., 2003). A few causalities were observed due to the transfusion of blood samples warmed in a microwave oven due to the lysis of the warmed blood caused by the over-heating at particular places like edges, tips of the blood bag, etc. (Herron et al., 1997; Schwaitzberg et al., 1991). Hence, the modeling of the microwave facilitated blood sample warming was encouraged with an aim to analyze the role of different factors affecting the procedure and to design techniques to circumvent over-heating and reduce the damage to blood samples (Herron et al., 1997; Schwaitzberg et al., 1991). The mathematical modeling of the microwave facilitated blood warming procedure is a very complex work due to highly non-linear interaction of the microwave radiation with blood samples. The demand for large quantity of warm blood during any massive transfusion urges for a meticulous study on the microwave facilitated homogenous and rapid warming of blood sample using the volumetric processing property of the radiation (Kumari and Samanta, 2022b; Schwaitzberg et al., 1991).

In the present work, the aim was to set the parameters required to design a mono-mode microwave blood and other intravenous fluid warmer which could be sensitive to temperature. The human blood was assumed to be placed inside a mono-mode microwave warmer and in a cylindrical container working on two ISM (industrial, scientific and medical) frequencies $f = 915$ and 2450 MHz and three incident intensities $I_0 = 1.5, 2$ and $2.5 \text{ W}\cdot\text{cm}^{-2}$ of microwave radiation. The human blood samples of different sizes (diameter) were put through two very different interaction schemes i.e., lateral (sample with no rotation) and radial irradiations (sample with rotation). For any specific procedure, the detailed analysis was performed on the warming rate and thermal non-homogeneity of the blood sample by studying the trend of the average temperature and temperature difference versus time, respectively. Finally, the optimal warming strategy was recommended on the basis of higher warming rate and thermal homogeneity displayed by the procedure.

2. THEORETICAL FORMULATION

2.1. Calculation of power and temperature absorption

The information of distribution of heat/temperature inside the human blood being warmed was calculated based on the evaluation of the absorbed microwave radiation using the electromagnetic wave equation and the coupled energy balance equation. The evaluation of the extent of the microwave radiation absorption aids in the calculation of temperature distribution based on different techniques of the radiation interacting

with the sample i.e., lateral and radial irradiations. The technique of lateral interaction of the microwave radiation with the blood samples considers a single directional (left in this study) interaction assuming the sample to remain stationary in the plane wave. The radial interaction mode considers the sample being irradiated from all the directions uniformly from a coaxial cylindrical microwave source situated at infinity for analyzing the thermal effect when the sample may undergo rotation in the plane wave. The direction of the propagation of the microwave radiation i.e., z , is the direction in which the magnitude of the field radiation varies as shown in Figure 1. The Maxwell's equation given by

$$\nabla^2 E_x + \kappa^2 E_x = 0 \tag{1}$$

governs the propagation of microwave radiation due to the electric field (Ayappa et al., 1992). The propagation constant (κ) is comprised of dielectric constant (κ'), dielectric loss (κ'') of the human blood sample, radiation frequency and speed of light. The value of propagation constant is evaluated by

$$\kappa = \frac{2\pi f}{c} \sqrt{\kappa' + i\kappa''} \tag{2}$$

The Poynting theorem that provides the effective value of the dissipation of the local power (P) occurring inside the human blood sample is given by (Ayappa et al., 1992)

$$P = -\text{Re}(\nabla \cdot S) = \frac{1}{2} \omega \epsilon_0 \kappa'' E_x \cdot E_x^* \tag{3}$$

Integrating the above equation over the considered domain gives the average power absorbed as:

$$P_{av} = \frac{1}{S} \iint_{\Gamma} P(\Omega) d\Omega \tag{4}$$

where, S is the cross-sectional area of the cylindrical meat sample with Γ being the outer surface.

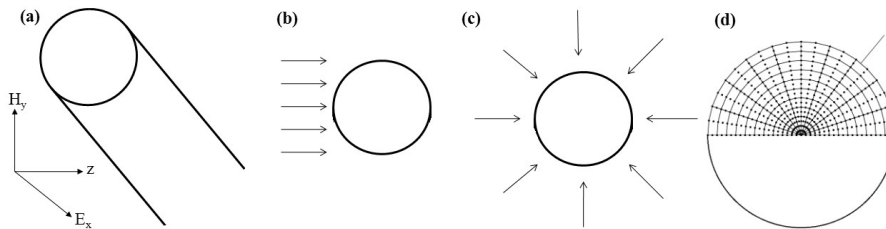


Fig. 1. The geometrical representation of the human blood sample and coordinates in (a) uniform plane waves, (b) lateral and (c) radial interaction technique; (d) mesh domain

The heat equation of the system describes the situation of heat conduction occurring inside the sample and also contains a heat generation term. The generation of heat in the human blood sample is related to the dissipation of power occurrence inside the sample i.e., P . The resulting equation for heat balance is given by

$$\rho C_p \frac{\partial T}{\partial t} = \nabla \cdot (k \nabla T) + P \tag{5}$$

The density (ρ), thermal conductivity (k) and specific heat (C_p) of the human blood sample are the thermal properties and assumed to be temperature-independent.

2.2. Calculation strategies and parameters

The entire two-dimensional geometry (circular cross-sectional surface) of the cylindrical sample was bifurcated in two horizontal parts. The boundary condition given by Keller and Givoli (1989) for scattered radiation pattern is imposed on a cylindrically shaped surface around the sample i.e., surface of the

cylinder in this case (see Fig. 1) (Keller and Givoli, 1989). The sample was assumed to be isotropic in nature and homogenous in terms of structure and properties throughout the sample. The computation was only performed on one half (upper half) of the bifurcated domain along with the pertinent boundary conditions. No flux condition (insulation condition) for outer surface has also been assumed.

The electric field propagation equation and the resultant heat equation were synchronously evaluated by applying the Galerkin finite element technique. The discretization of the time domain was performed by applying the Crank–Nicholson technique and the Newton–Raphson technique was applied to solve the non-linear residual equations. The Newton–Raphson technique was initialized using a very small time step of $1 \cdot 10^{-4}$ second for the first step and the successive time steps were of 0.1 second. A test for grid independence of the solution was performed on 100, 144 and 156 bi-quadratic elements for the entire study domain to observe very negligible differences. The modelling and simulation were performed using in-house FORTRAN code and MATLAB. The initial temperature of the human blood and the reference temperature for the study were decided such that both were set as 275 K. The dielectric and thermal properties of the human blood at desired frequencies were acquired from the available literature (Komarov et al., 2005).

3. RESULTS AND DISCUSSION

3.1. Warming of human whole blood at 915 MHz frequency

The microwave facilitated warming of cylindrically shaped human whole blood at frequency 915 MHz using both the lateral and radial interaction techniques was studied. The change in the absorption of power for the samples of different sizes at intensity $I_0 = 1.5 \text{ W}\cdot\text{cm}^{-2}$ was plotted (see Fig. 2(a)). The PP: 1 was selected at $d_c = 2.81 \text{ cm}$ due to the occurrence of a peak for the lateral interaction with $P_{av} = 1.01 \text{ W}\cdot\text{cm}^{-3}$ and subsequently the same point was also marked for the radial interaction with $P_{av} = 1.44 \text{ W}\cdot\text{cm}^{-3}$ for

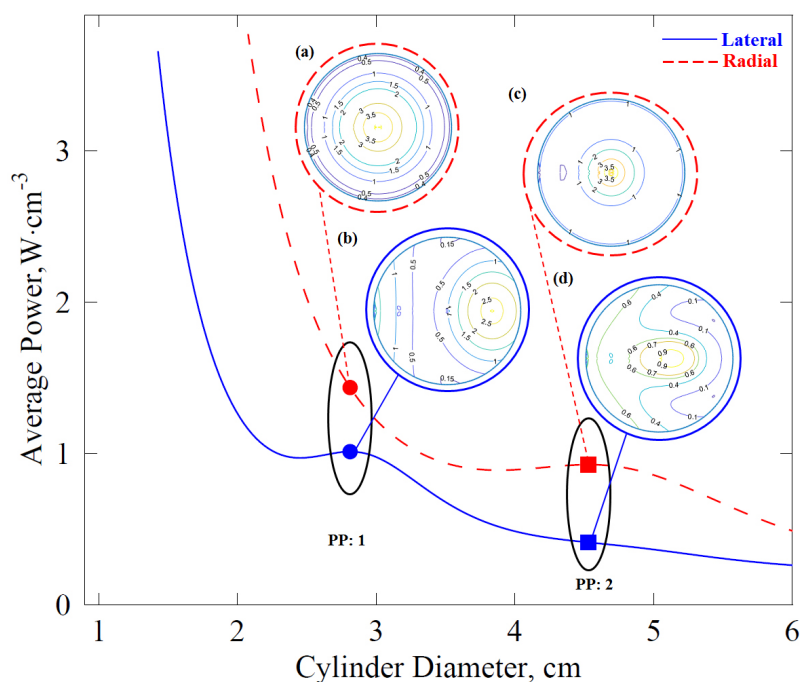


Fig. 2. Average power absorption ($\text{W}\cdot\text{cm}^{-3}$) versus sample diameter (cm) at $f = 915 \text{ MHz}$ and $I_0 = 1.5 \text{ W}\cdot\text{cm}^{-2}$. Inset: Areal power distribution for (a) radial warming at $d_c = 2.81 \text{ cm}$, (b) lateral warming at $d_c = 2.81 \text{ cm}$, (c) radial warming at $d_c = 4.53 \text{ cm}$, (d) lateral warming at $d_c = 4.53 \text{ cm}$

the purpose of comparative investigation and selection of the better interaction technique. Similarly, the next peak i.e., PP: 2 occurred at $d_c = 4.53$ cm for the radial interaction with $P_{av} = 0.93$ W·cm⁻³ and at the same sample size the lateral interaction showed $P_{av} = 0.41$ W·cm⁻³. The highs were reasoned to be the effects of the constructive interferences between the travelling waves (transmitted and reflected). The areal distribution of power at PP: 1 exhibited two maxima of 2.65 W·cm⁻³ at the right face and 2 W·cm⁻³ at the left face of the sample with the lateral interaction whereas it exhibited one maximum of 3.82 W·cm⁻³ at the radial centre of the sample with the radial interaction. The power minima of 0.14 and 0.37 W·cm⁻³ were observed for the lateral and radial interaction techniques, respectively at PP: 1. Similarly, at PP: 2, the areal distributions of power for the lateral and radial interaction techniques showed maxima of 0.98 and 3.68 W·cm⁻³ at the centre of the sample, respectively and minima of 0 and 0.34 W·cm⁻³, respectively.

The areal distribution of temperature in Figure 3(a), when the sample was subjected to the microwave radiation (at $f = 915$ MHz and $I_0 = 1.5$ W·cm⁻²) for the duration of 60 seconds at PP: 1, showed two high temperature cruxes of 306.97 K on the right side and 290 K on the left side along with the minimum temperature of 278.97 K for the lateral interaction. In addition, the temperature maximum of 320.8 K at the centre and the minimum of 284.98 K were observed for the radial interaction at PP: 1 for the same time duration. For the duration of 60 seconds at PP: 2, the areal maxima of the temperature contour obtained were 287.26 and 319.07 K at the centre of the sample for the lateral and radial interactions, respectively. In addition, the temperature minima were 275.34 and 282.31 K for the lateral and radial interactions, respectively.

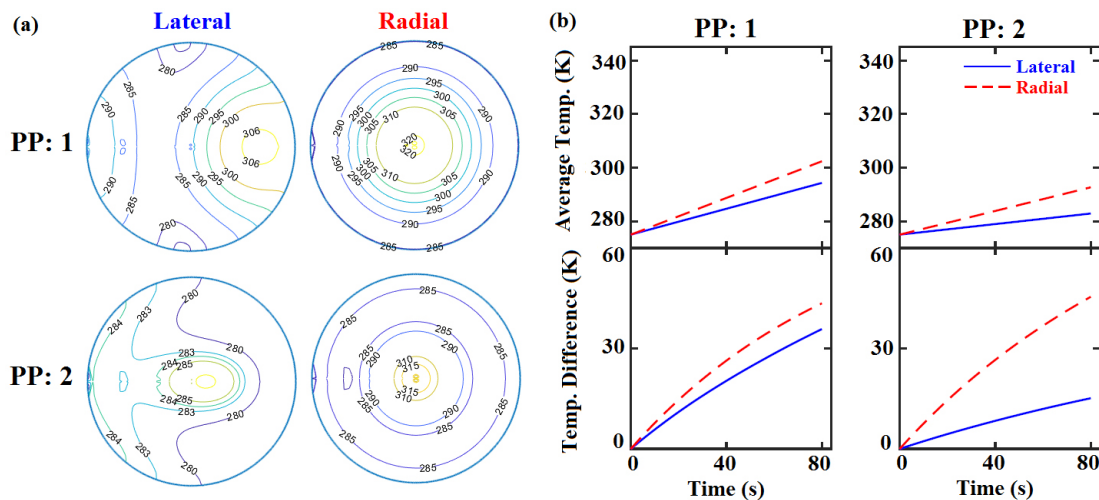


Fig. 3. Areal temperature distribution at $f = 915$ MHz and $I_0 = 1.5$ W·cm⁻² during interaction duration of 60 s. (b) [Top] Average temperature (K) versus time (s); [Bottom] Temperature difference (K) versus time (s)

The plots in Figure 3(b) showed that the radial interaction for both PP: 1 and 2 led to higher warming rate than those with the lateral interaction at $f = 915$ MHz and $I_0 = 1.5$ W·cm⁻². However, owing to the fact that the human blood used to be very delicate in nature and prone to denaturation on exposure to high temperatures, the lateral interaction was the preferred technique due to higher homogeneity in temperature distribution for both the PPs. Therefore, the lateral interaction technique was recommended to achieve good warming with reasonable thermal uniformity for PP: 1. Hence, sample rotation was not required in this case. On the other hand, despite having higher thermal homogeneity the lateral interaction was not recommended due to a very low warming rate for PP: 2. Hence, none of the interaction techniques was recommended eventually at this radiation intensity and frequency for large samples.

To study the effect of intensity, we warmed the human blood at an increased intensity of $I_0 = 2.5$ W·cm⁻² keeping the same frequency at 915 MHz. The thermal effect of the microwave interaction with the human blood at the mentioned condition in terms of absorption of average power was studied (figure not shown). The average powers for the lateral interaction technique at PP: 1 ($d_c = 2.81$ cm) and PP: 2 ($d_c = 4.53$ cm)

were $P_{av} = 1.69$ and $0.69 \text{ W}\cdot\text{cm}^{-3}$, respectively whereas those for the radial interaction at PP: 1 and 2 were $P_{av} = 2.4$ and $1.55 \text{ W}\cdot\text{cm}^{-3}$, respectively. The maxima in areal power during the lateral interaction at PP: 1 were $2 \text{ W}\cdot\text{cm}^{-3}$ on the left side and $4.42 \text{ W}\cdot\text{cm}^{-3}$ on the right side. At PP: 2, the maximum in areal power of $1.64 \text{ W}\cdot\text{cm}^{-3}$ was observed at the centre of the sample for the lateral interaction. For the radial interaction, the maxima in areal powers of 6.37 and $6.13 \text{ W}\cdot\text{cm}^{-3}$ were observed at the centre of the sample for PP: 1 and 2, respectively.

Studying the warming rate and thermal homogeneity for PP: 1, it was observed that both the lateral and radial interaction techniques exhibited extremely high non-homogenous distribution of temperature (figure not shown). Hence, none of the techniques was preferred for this PP. At larger sample size i.e., for PP: 2, the lateral interaction though showed a slightly lower warming rate but it ensured extremely controlled thermal homogeneity. Hence, the lateral interaction technique was preferred for PP: 2 and that recommended no rotation requirement for the warming of large samples.

3.2. Warming of human whole blood at 2450 MHz frequency

Further, human blood was warmed at 2450 MHz frequency at different intensities and for different time durations for analyzing the selection of best warming technique between the lateral and radial interactions. The microwave facilitated warming of human blood at 2450 MHz frequency with an incident radiation intensity of $I_0 = 2 \text{ W}\cdot\text{cm}^{-2}$ exhibited few peaks for the average power absorption inside the human blood with respect to its different sizes (see Fig. 4). The first peak point i.e., PP: 1 was recognized corresponding to $d_c = 1.15 \text{ cm}$ which exhibited the average power absorptions (P_{av}) of about 4.01 and $3.22 \text{ W}\cdot\text{cm}^{-3}$ for the lateral and radial interactions, respectively. Similarly, PP: 2 was obtained corresponding to $d_c = 1.89 \text{ cm}$ and exhibited average power absorptions of about 1.37 and $3.53 \text{ W}\cdot\text{cm}^{-3}$ for the lateral and radial interactions, respectively. In addition, PP: 3 corresponding to $d_c = 3.38 \text{ cm}$ showed average power absorptions of about 0.53 and $0.82 \text{ W}\cdot\text{cm}^{-3}$ for the lateral and radial interactions, respectively. Note that, PP: 1 demonstrated higher absorption of average power for the lateral interaction technique whereas PP: 2 and PP: 3 demonstrated higher absorption of average power for the radial interaction technique.

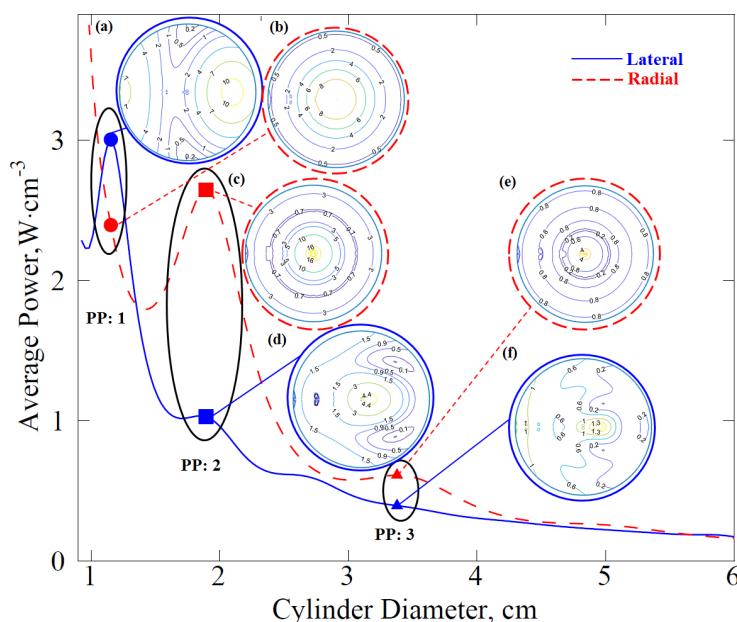


Fig. 4. Average power absorption ($\text{W}\cdot\text{cm}^{-3}$) versus sample diameter (cm) at $f = 2450 \text{ MHz}$ and $I_0 = 2 \text{ W}\cdot\text{cm}^{-2}$. Inset: Areal power distribution for (a) lateral warming at $d_c = 1.15 \text{ cm}$, (b) radial warming at $d_c = 1.15 \text{ cm}$, (c) radial warming at $d_c = 1.89 \text{ cm}$, (d) lateral warming at $d_c = 1.89 \text{ cm}$, (e) radial warming at $d_c = 3.38 \text{ cm}$, (f) lateral warming at $d_c = 3.38 \text{ cm}$

The insets of Figure 4 exhibited areal power distribution inside the human blood corresponding to the respective PPs and interaction techniques. The contour of power distribution for the lateral interaction corresponding to PP: 1 showed two power maxima, one on the right side with maximum power of about $10.86 \text{ W}\cdot\text{cm}^{-3}$ and another on the left side with maximum power of about $7 \text{ W}\cdot\text{cm}^{-3}$, whereas the power at the centre depicting the minimum absorption of power ranged around $0.18 \text{ W}\cdot\text{cm}^{-3}$ as shown in Figure 4(a). In addition, PP: 2 for the lateral mode of interaction demonstrated the power maximum of $4.77 \text{ W}\cdot\text{cm}^{-3}$ at the centre along with the minimum of about $0 \text{ W}\cdot\text{cm}^{-3}$ (see Fig. 4(d)). Similarly, PP: 3 for the lateral interaction exhibited the maximum power of $1.47 \text{ W}\cdot\text{cm}^{-3}$ at the centre of the sample and minimum power of about $0 \text{ W}\cdot\text{cm}^{-3}$ as shown in Figure 4(f). On observing the power distribution for the radial interaction technique corresponding to all the 3 PPs, centrally positioned power maxima were obtained which were decreased on moving towards the outer edge of the blood samples as shown in Figure 4(b), 4(c) and 4(e). Note that, the power maxima for the radial interaction technique were found to be of about 10.01, 17.42 and $4.66 \text{ W}\cdot\text{cm}^{-3}$ for PP: 1, 2 and 3, respectively (Fig. 4(b), 4(c) and 4(e)).

Figure 5(a) exhibited the areal distribution of temperature for blood samples corresponding to PP: 1, 2 and 3 on 20 seconds exposure of the microwave radiation of intensity $2 \text{ W}\cdot\text{cm}^{-2}$. The lateral interaction for PP: 1 exhibited two temperature maxima of about 314.92 and 300 K on the right and the left side of the blood sample, respectively along with the minimum temperature of about 280.92 K. On the other hand, the radial mode exhibited a centrally positioned temperature maximum of about 308.44 K and a minimum of about 282.91 K for PP: 1. For PP: 2, the temperature maximum of about 291.45 K was observed at the centre of the sample along with the minimum of about 276.21 K for the lateral interaction. Note that, the central maximum of 333.16 K and minimum of 284.7 K for the radial interaction were observed for PP: 2. In addition, for PP: 3, the lateral interaction displayed a central maximum of about 280.42 K whereas the radial interaction demonstrated a central maximum of about 290.59 K. Note that, the temperature minima of 275.15 and 277.66 K were observed for the lateral and radial interactions, respectively for PP: 3.

Figure 5(b) displayed the warming rate and thermal non-homogeneity during the microwave facilitated warming of the human blood sample corresponding to PP: 1, 2 and 3. Note that, the radial interaction was found as the desired warming technique for PP: 1 since it demonstrated a good warming rate and very high thermal homogeneity. On the other hand, the lateral interaction was preferred for PP: 2 due to higher thermal homogeneity and a moderate warming rate. However, for PP: 3, the warming rate was very low for both the interaction techniques. Hence, none of the interaction techniques was recommended for large

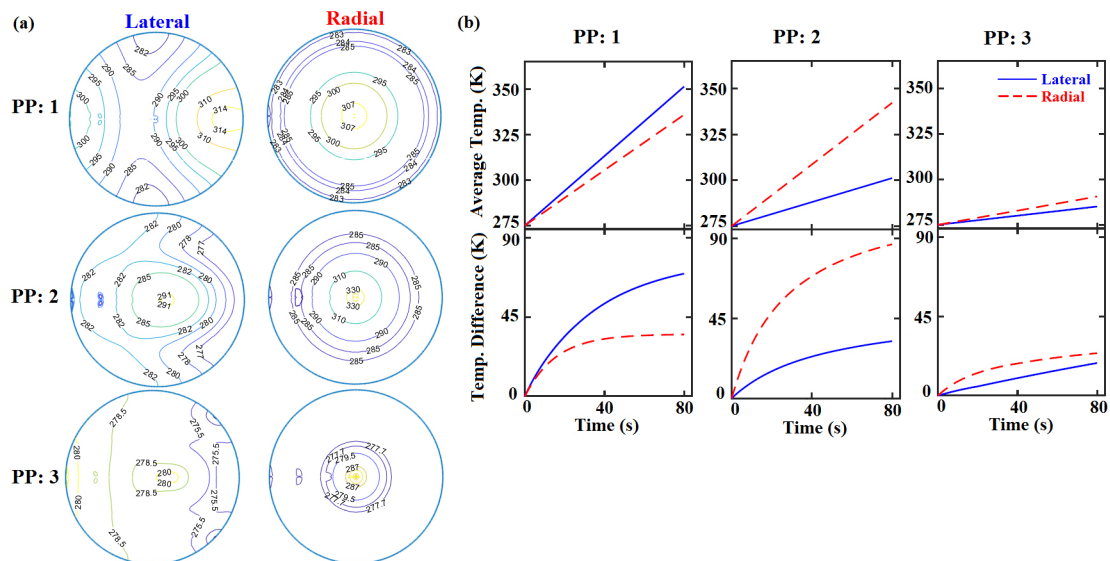


Fig. 5. Areal temperature distribution at $f = 2450 \text{ MHz}$ and $I_0 = 2 \text{ W}\cdot\text{cm}^{-2}$ during interaction duration of 20 s; (b) [Top] Average temperature (K) versus time (s); [Bottom] Temperature difference (K) versus time (s)

samples. Hence, small samples required rotation and medium sized samples did not require any rotation to achieve thermal homogeneity with a good warming rate.

Figure 5(b) displayed the warming rate and thermal non-homogeneity during the microwave facilitated warming of the human blood sample corresponding to PP: 1, 2 and 3. Note that the radial interaction was found as the desired warming technique for PP: 1 since it demonstrated a good warming rate and very high thermal homogeneity. On the other hand, the lateral interaction was preferred for PP: 2 due to higher thermal homogeneity and a moderate warming rate. However, for PP: 3, the warming rate was very low for both the interaction techniques. Hence, none of the interaction techniques was recommended for large samples. Hence, small samples required rotation and medium sized samples did not require any rotation to achieve thermal homogeneity with a good warming rate.

3.3. Comparison of the warming effects at 915 and 2450 MHz frequencies

In order to choose a better frequency between 915 and 2450 MHz, the warming rate and thermal homogeneity of the procedure at both 915 and 2450 MHz at incident radiation intensity of $2 \text{ W}\cdot\text{cm}^{-2}$ and for different sample sizes were studied (figure not shown). For the small sample size, we observed that both the interaction techniques exhibited very high thermal non-homogeneity during the warming at 915 MHz frequency. Hence, none of the techniques was recommended. In contrast, the warming rate was slightly higher during the radial interaction and the thermal homogeneity was almost same within acceptable limits for both interaction techniques, leading to the radial interaction technique being the preferred warming technique at 2450 MHz frequency. Proceeding to the selection of better frequency between 915 and 2450 MHz, we observed warming at 2450 MHz to exhibit better thermal homogeneity with a suitable warming rate at sample size of 2.7 cm.

915 MHz frequency, although the lateral interaction technique showed slightly lower warming rate but due to relatively better and acceptable thermal non-homogeneity, was preferred as the optimum warming strategy at increased sample size (figure not shown). In contrast, the radial interaction technique exhibited not only a higher warming rate but also better thermal homogeneity making it the preferred technique at 2450 MHz. On comparison between 915 and 2450 MHz, it was observed that both the frequencies corresponded to an almost similar good warming rate for 3.7 cm sample. However, 2450 MHz showed better thermal homogeneity. Hence, 2450 MHz was the preferred frequency for the warming of human blood since the blood sample used to be highly delicate in nature and prone to denaturation on being subjected to high thermal non-homogeneities. Moreover, the discussion of human blood warming at 915 MHz in the above section already indicated its inability towards proper warming of small samples.

3.4. Analyzing the reciprocity between procedure duration and radiation intensity for obtaining thermal homogeneity

Reverting to the issue of occurrence of thermal non-homogeneity, we tried to strike a balance between intensity and procedure duration. The authors tried the warming at different time intervals to see if the non-homogeneity could be reduced along with maintaining a good warming rate and observed very interesting behaviors. For 915 MHz frequency, the cases of identical extent of warming (average temperature) at $I_0 = 1.5 \text{ W}\cdot\text{cm}^{-2}$ for time duration $t = 80 \text{ s}$ and at $I_0 = 2 \text{ W}\cdot\text{cm}^{-2}$ for $t = 60 \text{ s}$, exhibited slightly higher thermal non-homogeneity (temperature difference) at higher intensity. Likewise, with higher thermal non-homogeneity at $I_0 = 2.5 \text{ W}\cdot\text{cm}^{-2}$, the extent of warming at $I_0 = 2 \text{ W}\cdot\text{cm}^{-2}$ for $t = 50 \text{ s}$ and $I_0 = 2.5 \text{ W}\cdot\text{cm}^{-2}$ for $t = 40 \text{ s}$ was similar. This indicated a pattern of comparable warming extent for higher intensity at lesser time but with higher thermal non-homogeneity.

A similar study was performed at 2450 MHz to obtain a good balance between intensity of radiation and procedure duration corresponding to the interaction technique applied. It was observed that for the cases of identical extent of warming, higher intensity required lesser procedure duration. However, the thermal homogeneity was found better at lower intensity. For instance, the extent of warming (average temperature) for $I_0 = 1.5 \text{ W}\cdot\text{cm}^{-2}$ at time duration i.e., $t = 40 \text{ s}$ and $I_0 = 2 \text{ W}\cdot\text{cm}^{-2}$ at $t = 30 \text{ s}$ were identical. However, the thermal non-homogeneity (temperature difference) was higher for $I_0 = 2 \text{ W}\cdot\text{cm}^{-2}$. This interesting observation indicated better thermal homogeneity at lower microwave intensity with a similar extent of warming but with longer procedure duration.

4. CONCLUSIONS

The study was conducted to understand the reciprocity between the different parameters to aid the designing of the prototype mono-mode microwave blood warmer. The optimal interdependency of parameters to achieve homogeneously and rapidly warmed human blood (placed in a cylindrical container) using microwave radiation was analyzed. The analysis was aimed to select the optimum warming technique amongst the lateral and radial interaction techniques to decide the necessity of sample rotation. At 915 MHz, non-rotational (lateral interaction) technique was preferred for samples with ~ 2.81 and ~ 4.53 cm diameters corresponding to $I_0 = 1.5$ and $2.5 \text{ W}\cdot\text{cm}^{-2}$, respectively. At 2450 MHz frequency, rotational (radial interaction) technique was preferred for both samples with ~ 1.15 and ~ 3.38 cm diameters for all intensities. However, non-rotational (lateral interaction) technique was preferred for samples with ~ 1.89 cm diameter for all intensities. Some uncertainties were also observed due to cases of a very low heating rate or very high thermal non-homogeneity where none of the interaction schemes was recommended. Furthermore, between 915 and 2450 MHz frequency, the latter was preferred owing to a good warming rate and thermal homogeneity for all the cases of sizes and radiation intensities. The detailed analysis on the reciprocity between radiation intensity and procedure duration was also discussed. It was observed that better thermal homogeneity could be obtained at lower microwave radiation intensity with a similar extent of warming on increasing the procedure duration. Finally, we concluded that the behavior of an efficient interaction technique used for the warming procedure depended on the dielectric properties of the blood sample, the duration of interaction of the radiation with the sample, the frequency and intensity of the radiation along with the sample rotation requirement and the present study provided the pertinent guidelines and recommendations for the selection of optimum combinations. These detailed interdependencies of the parameters would aid the designing of mono-mode blood warmers with some pre-set calibrated features for swift and homogeneous warming.

The authors would also like to acknowledge and thank the administration of Indian Institute of Technology Patna for providing the assistances required for this study.

SYMBOLS

E_x	electric field intensity, $\text{V}\cdot\text{m}^{-1}$
E_x^*	conjugate electric field intensity, $\text{V}\cdot\text{m}^{-1}$
H_y	magnetic field, $\text{A}\cdot\text{m}^{-1}$
κ	propagation constant, –
κ'	dielectric constant, –
κ''	dielectric loss, –
f	frequency, Hz

c	speed of light, $\text{m}\cdot\text{s}^{-1}$
ρ	density, $\text{kg}\cdot\text{m}^{-3}$
C_p	specific heat capacity, $\text{J}\cdot\text{kg}^{-1}\cdot\text{K}^{-1}$
k	thermal conductivity, $\text{W}\cdot\text{m}^{-1}\cdot\text{K}^{-1}$
P_{av}	average power, $\text{W}\cdot\text{m}^{-3}$
Γ	outer surface of sample, m^2
S	cross-sectional area of the cylindrical sample, m^2
ϵ_0	free space permittivity, $\text{F}\cdot\text{m}^{-1}$
μ_0	free space permeability, $\text{H}\cdot\text{m}^{-1}$

REFERENCES

- Ayappa K.G., Davis H.T., Davis E.A., Gordon J., 1992. Two-dimensional finite element analysis of microwave heating. *AIChE J.*, 38, 1577–1592. DOI: [10.1002/aic.690381009](https://doi.org/10.1002/aic.690381009).
- Boyan C.P., 1964. Cold or warmed blood for massive transfusions. *Annals Surgery*, 160, 282–286. DOI: [10.1097/0000658-196408000-00016](https://doi.org/10.1097/0000658-196408000-00016).
- Custer B., Zou S., Glynn S.A., Makani J., Tayou Tagny C., El Ekiaby M., Sabino E.C., Choudhury N., Teo D., Nelson K., Peparah E., 2018. Addressing gaps in international blood availability and transfusion safety in low-and middle-income countries: A NHLBI workshop. *Transfusion*, 58, 1307–1317. DOI: [10.1111/trf.14598](https://doi.org/10.1111/trf.14598).
- Frazier S.K., Higgins J., Bugajski A., Jones A.R., Brown M.R., 2017. Adverse reactions to transfusion of blood products and best practices for prevention. *Crit. Care Nurs. Clin. North Am.*, 29, 271–290. DOI: [10.1016/j.cnc.2017.04.002](https://doi.org/10.1016/j.cnc.2017.04.002).
- Herron D.M., Grabowy R., Connolly R., Schwaitzberg S.D., 1997. The limits of bloodwarming. Maximally heating blood with an inline microwave bloodwarmer. *J. Trauma Acute Care Surg.*, 43, 219–228. DOI: [10.1097/00005373-199708000-00003](https://doi.org/10.1097/00005373-199708000-00003).
- Hirsch J., Menzebach A., Welters I.D., Dietrich G.V., Katz N., Hempelmann G., 2003. Indicators of erythrocyte damage after microwave warming of packed red blood cells. *Clin. Chem.*, 49, 792–799. DOI: [10.1373/49.5.792](https://doi.org/10.1373/49.5.792).
- Keller J.B., Givoli D., 1989. Exact non-reflecting boundary conditions. *J. Comput. Phys.*, 82, 172–192. DOI: [10.1016/0021-9991\(89\)90041-7](https://doi.org/10.1016/0021-9991(89)90041-7).
- Komarov V., Wang S., Tang J., 2005. Permittivity and measurements. *Encyclopedia of RF and Microwave Engineering*, 1–20. DOI: [10.1002/0471654507.eme308](https://doi.org/10.1002/0471654507.eme308).
- Kumari S., Samanta S.K., 2020. 1D study on microwave assisted warming of human blood with varied ceramic and composite supports. *J. Indian Chem. Soc.*, 97, 379–383.
- Kumari S., Samanta S.K., 2022. The effect of temperature and additives on the dielectric behavior of human whole blood, its different components and cell suspensions. *IEEE Trans. Instrum. Meas.*, 71, 1–9, 1001809. DOI: [10.1109/TIM.2022.3141078](https://doi.org/10.1109/TIM.2022.3141078).
- Kumari S., Samanta S.K., 2022. The evolution of microwave assisted thermal processing of pre-transfusion human blood: A review. *Materials Today: Proceedings*, 57, 1877–1883. DOI: [10.1016/j.matpr.2022.01.196](https://doi.org/10.1016/j.matpr.2022.01.196).
- Lubner M.G., Brace C.L., Hinshaw J.L., Lee F.T., 2010. Microwave tumor ablation: Mechanism of action, clinical results, and devices. *J. Vasc. Interventional Radiol.*, 21(SUPPL. 8), S192–S203. DOI: [10.1016/j.jvir.2010.04.007](https://doi.org/10.1016/j.jvir.2010.04.007).
- Nair S.S., Sreedevi V., Nagesh D.S., 2021. Warming of blood and intravenous fluids using low-power infra-red light-emitting diodes. *J. Med. Eng. Technol.*, 45, 614–626. DOI: [10.1080/03091902.2021.1936675](https://doi.org/10.1080/03091902.2021.1936675).
- Poder T.G., Pruneau D., Dorval J., Thibault L., Fiset J., Bédard S.K., Jacques A., Beaugard P., 2016. Effect of warming and flow rate conditions of blood warmers on red blood cell integrity. *Vox Sanguinis*, 111, 341–349. DOI: [10.1111/vox.12423](https://doi.org/10.1111/vox.12423).

- Poder T.G., Pruneau D., Dorval J., Thibault L., Fiset J.-F., Bédard S.K., Jacques A., Beauregard P., 2016. Pressure infusion cuff and bloodwarmer during massive transfusion: An experimental study about hemolysis and hypothermia. *PLOS ONE*, 11, e0163429. DOI: [10.1371/journal.pone.0163429](https://doi.org/10.1371/journal.pone.0163429).
- Rosen A., Stuchly M.A., Vander Vorst A., 2002. Applications of RF/microwaves in medicine. *IEEE Trans. Microwave Theory Tech.*, 50, 963–974. DOI: [10.1109/22.989979](https://doi.org/10.1109/22.989979).
- Samanta S.K., Basak T., 2008. Theoretical analysis of efficient microwave processing of oil-water emulsions attached with various ceramic plates. *Food Res. Int.*, 41, 386–403. DOI: [10.1016/j.foodres.2008.01.003](https://doi.org/10.1016/j.foodres.2008.01.003).
- Samanta S.K., Basak T., 2009. Efficient microwave processing of oil-water emulsion cylinders with lateral and radial irradiations. *Food Res. Int.*, 42, 1337–1350. DOI: [10.1016/j.foodres.2009.06.010](https://doi.org/10.1016/j.foodres.2009.06.010).
- Samanta S.K., Basak T., 2010. Efficient processing of oil-water emulsions confined within 2D cylinders with various microwave irradiations: Role of metallic annulus. *Food Res. Int.*, 43, 148–166. DOI: [10.1016/j.foodres.2009.09.015](https://doi.org/10.1016/j.foodres.2009.09.015).
- Schwaitzberg S.D., Allen M.J., Connolly R.J., Grabowy R.S., Carr K.L., Cleveland R.J., 1991. Rapid in-line blood warming using microwave energy: preliminary studies. *J. Investigative Surg.*, 4, 505–510. DOI: [10.3109/08941939109141182](https://doi.org/10.3109/08941939109141182).
- Smith C.E., Wagner K.G., 2008. Principles of fluid and blood warming in trauma. *International Trauma Care (ITACCS)*, 18, 71–79.
- Storch E.K., Custer B.S., Jacobs M.R., Menitove J.E., Mintz P.D., 2019. Review of current transfusion therapy and blood banking practices. *Blood Rev.*, 38, 100593. DOI: [10.1016/j.blre.2019.100593](https://doi.org/10.1016/j.blre.2019.100593).
- Vrba J., 2005. Medical applications of microwaves. *Electromagn. Biol. Med.*, 24, 441–448. DOI: [10.1080/15368370500382214](https://doi.org/10.1080/15368370500382214).
- Zimrin A.B., Hess J.R., 2009. Current issues relating to the transfusion of stored red blood cells. *Vox Sanguinis*, 96, 93–103. DOI: [10.1111/j.1423-0410.2008.01117.x](https://doi.org/10.1111/j.1423-0410.2008.01117.x).

Received 16 February 2022

Received in revised form 22 March 2022

Accepted 6 April 2022